Channel-interacting PDZ protein "CIPP" interacts with proteins involved in cytoskeletal dynamics

Emanuele Alpi, Elena Landi, Manuela Barilari, Michela Serresi, Piero Salvadori, Angela Bachi, Luciana Dente

Channel-interacting PDZ protein "CIPP" interacts with proteins involved in cytoskeletal dynamics

Emanuele ALPI*†[1], Elena LANDI*[1], Manuela BARILARI*[1], Michela SERRESI‡, Piero SALVADORI§, Angela BACHI‖ and Luciana DENTE*[2]

** Cell and Developmental Biology Laboratory, Department of Biology, University of Pisa, 56010 Pisa, Italy; † Molecular Biology Laboratory, Scuola Normale Superiore, 56124 Pisa, Italy; ‡ NEST Scuola Normale Superiore and IIT, 56126 Pisa, Italy; § Department of Chemistry and Industrial Chemistry, University of Pisa, 56126 Pisa, Italy; ‖ Dibit2 - San Raffaele Scientific Institute, 20132 Milano, Italy*

[1] First three authors contributed equally to this work

[2] To whom correspondence should be addressed: Prof. Luciana Dente, Laboratori di Biologia Cellulare e dello Sviluppo, Dipartimento di Biologia, Università of Pisa, via Carducci 13, Ghezzano-Pisa 56010, Italy. Tel. +390502211488; Fax: +390502211495; E-mail: ldente@biologia.unipi.it

Short title (page heading): Cytosolic interactors of CIPP protein

SYNOPSIS

Neuronal CIPP is a multivalent PDZ protein that interacts with specific channels and receptors, highly expressed in the brain. It is composed of four PDZ domains that behave as a scaffold to clusterize functionally connected proteins. In this study, we selected a set of potential CIPP interactors that are directly or indirectly involved in mechanisms of cytoskeletal remodeling and membrane protrusions formation. For some of these, we first proved the direct binding to specific CIPP PDZ domains considered as autonomous elements, and then confirmed the interaction with the whole protein. In particular, the small G-protein effector IRSp53 (insulin receptor tyrosine kinase substrate protein p53) specifically interacts with the second PDZ domain of CIPP and, when co-transfected in mammalian cultured cells with a tagged full-length CIPP, it induces a marked reorganization of CIPP cytoplasmic localization. Large punctate structures are generated as a consequence of CIPP binding to IRSp53 carboxy-terminus. Analysis of the puncta nature, using various endocytic markers, revealed that they are not related to cytoplasmic vesicles, rather represent multi-protein assemblies, where CIPP can tether other potential interactors.

Key words: multi-PDZ proteins, IRSp53, Cypin, endocytosis, actin tubulin remodeling.

Abbreviations used: PDZ, PSD-95 Dlg ZO-1; IRSp53, insulin receptor tyrosine kinase substrate protein p53; CNP, 2',3'-cyclic-nucleotide 3'-phosphodiesterase; PATJ, Pals1 Associated Tight Junction protein; INADL, Inactivation-No Afterpotential D Like; PALS1, protein associated with Lin seven; CRB, Crumbs; NMDA, *N*-methyl-D-aspartate; MALDI-TOF, matrix assisted laser desorption/ionization time of flight; PMF, peptide mass fingerprint; GST, glutathione-S-transferase.

INTRODUCTION

Recognition and binding of specific proteins are crucial for the formation of multiprotein complexes that are fundamental for cell viability. Protein interaction networks are often mediated by specialized small binding domains, which are responsible for recognition specificity.

PDZ domains (**P**SD-95/**D**lg/**Z**O-1) belong to a family of widespread protein modules that function as "adapters" of multimeric complexes. A great number of PDZ domain interactions are known and most of them concern proteins containing multiple PDZ domains involved in cell adhesion, signal transduction and synapses organization at plasma membrane level (for recent reviews, see [1-4]).

Murine CIPP "channel-interacting PDZ protein" is a typical example of multi-PDZ protein, whose PDZ modules are engaged in recruiting different channels and receptors at membrane level [5]. Genomic mapping of the mouse transcriptome revealed a larger variety of alternative transcripts, deriving from the corresponding gene ID:1269, located on chromosome 4 [6]. The gene has different names: INADL, PATJ, CIPP, which are related to various protein isoforms with a different number of binding domains. The name INADL derives from a screening project aimed to find homologs of the multivalent INAD protein of *Drosophila melanogaster*; then again, part of the INADL sequence, containing eight PDZ domains, was found to share higher homology with DLT, a *Drosophila* protein involved in epithelial cell polarity [7-9]. Longer isoforms including up to ten PDZ domains were then renamed PATJ due to their association to the tight junctions in epithelial cells, via an amino-terminal MRE/L27 domain able to dimerize with the L27 domain of PALS1, a component of the CRB apical complex [8, 10, 11]. Finally, CIPP is a short isoform, mainly expressed in brain and kidney, containing only four PDZ domains, but missing the MRE/L27 domain. CIPP was identified as a potential partner of inward rectifier K^+ family channels, of *N*-methyl-D-aspartate receptors - NR2 subunits, and of cell surface molecules enriched in synaptic membranes such as neurexins and neuroligins [5]. Furthermore, it has been proposed that CIPP interacts with acid-sensing ion channel 3 (ASIC), a cationic channel activated by extracellular pH [12] and with different types of serotonin receptors and transporters [13-15]. All these findings suggest that, unlike longer isoforms associated to the tight junctions, CIPP may rather functions as a scaffold connecting different channels and receptors to cytosolic partners, which are currently unknown.

Here we have purified and identified a set of potential CIPP interacting proteins from cytoplasmic brain extracts using affinity chromatography and mass spectrometry. The majority of the selected interactors represent proteins somehow involved in actin and tubulin remodeling. In particular, we focused our study on the interaction of CIPP with IRSp53, a key player in cytoskeletal dynamics, also implicated in receptor-mediated plasticity [16, 17]. We observed that IRSp53, following PDZ-mediated interaction with CIPP, is able to induce the formation of large cytoplasmic assemblies that may include other co-transfected proteins. Our findings highlight possible functional roles of CIPP in cytoskeletal remodeling and provide tools for further molecular dissection of neural cell plasticity.

EXPERIMENTAL

Chemicals and antibodies

Reagents and solvents were from Sigma-Aldrich (St. Louis, MO), unless otherwise specified, and were of the highest purity grade. The following antibodies were used: mouse monoclonal anti-FLAG M2 peroxidase conjugate from Sigma; rabbit polyclonal anti-GFP from Invitrogen; monoclonal Anti-HA from Sigma. Trypsin for PMF was from Roche, bovine pancreas sequencing grade. The MALDI matrix material (α-cyano-4-hydroxy-trans-cinnamic acid, CHCA) was recrystallized in EtOH. For cell fluorescence microscopy we used anti goat EEA1 antibody (Santa Cruz) to label endosomes, anti mouse Lamp2 (BD Pharmingen) to label lysosomes, anti rabbit giantin (Babco) to stain the Golgi apparatus, anti mouse Clathrin Heavy Chain (ABR) to label clathrin coated vesicles, anti human

epidermal growth factor, hEGFR (Calbiochem) to label the membranes. Secondary antibodies: anti rabbit IgG (whole molecule) peroxidase conjugate from Sigma, produced in goat; anti mouse IgG peroxidase conjugate from Sigma. Antibodies conjugated with Alexa 647 fluorophore were purchased from Molecular Probes Invitrogen.

Plasmid construction

The coding regions of CIPP-PDZ domains were amplified by polymerase chain reaction from a full-length cDNA CIPP clone (accession number: BC057124) obtained from IMAGE consortium (n. 641366), using specific oligonucleotides designed to hybridize to the domain flanking regions: for PDZ1 5'CATTGGATCCCTGGAAAAGGACAAGAATG3', 5'GGCGAATTCACTGACTGCATCTTCGTTTC3'; for PDZ2 5'GATCGGATCCATATCCAAGGGACGCT3', 5'GTCGAATTCTCTGTACTGTGCTTCATCTC3'; for PDZ3 5'CGCGGATCCCTTGTGGACCTGCAGAAG3', 5'CTGGGAATTCTGCGAGGTCTTCCGAG3'; for PDZ4 5'GGAAGGATCCACTGTAGAGATAATCAGAG3', 5'GATGAATTCCTGGGTCGCTATGGCAC3'. The amplified fragments were directionally subcloned in pYex vector (a modified version of pGEX2T), in BamHI-EcoRI restriction sites. The corresponding recombinant proteins were all soluble and highly expressed in bacteria. The p3XFLAG-CMV-10 vector was used for FLAG-tagged constructs. The coding regions of CNP (amplified from IMAGE clone 3669076) and of IRSp53 S-isoform including the PDZ binding motif (amplified by RT-PCR from adult mouse brain RNA) were inserted between EcoRI and BamHI sites. The mutant N-mut IRSp53 was subcloned from IMAGE clone 5480221, cut with EcoRI and XmnI. The coding region of Cypin was subcloned from the IMAGE clone 5186337 cut with KpnI and HindIII either in p3XFLAG-CMV-10 or in HA-pcDNA (kind gift of A. Zucconi) vectors. Full-length CIPP (amplified from IMAGE clone 641366) was cloned between EcoRI and BamHI sites of pEGFP-C1 vector (Clontech). All expression constructs generated by PCR amplification were verified by automated sequence analysis to exclude undesired mutations. The primer sequences for CIPP were: 5'GTCGAATTCCATGGTCCACGGGGGCTTCCCAG3', 5'CTCGGATCCTCAGCTAAGATCTGGTCACTTCAC3'; for IRSp53: 5'CGCGAATTCGATGTCGCTTTCACGCTCGGAGGAGATGCACCGGCTCACGG3', 5'GCGGGATCCTCACACTGTGGACACCAGCGTGCCACTGCCACTGCTCAC3'; for CNP 5'TGCGGAATTCCATCATGAACACAAGCTTTAC3', 5'CGGTGGATCCCCTCAGATGATGGTGCAGATC3'. The mutagenic primer sequence for substituting the PDZ binding motif was: 5'GCGGGATCCTCACGATGGCGCCACCAGCGTGCC3'.

GST protein production and purification

GST-fusion proteins were expressed in *Escherichia coli* BL21, transformed with the appropriate constructs and purified following manufacturer's instructions (GE-Healthcare) with some modifications: cultures were grown to mid-log phase (OD_{600}=0.7) in Luria–Bertani medium at 37 °C, induced with 1.0 mM isopropyl thio-β-D-galactoside (IPTG), and grown for an additional 3 h. 50 ml of bacteria suspension were pelleted by centrifugation at 4000 g for 5 min and resuspended in 1 ml of lysis buffer: lysozyme 200 µg/mL; DTT 10 mM pH 5.2; protease inhibitor mix for general use from Sigma (AEBSF 2 mM, EDTA 1 mM, bestatin 130 µM, E-64 14 µM, leupeptin 1 µM, aprotinin 0.3 µM); Triton X-100 1% (v/v); MgCl2 10 mM; DNase I 100 µg/mL. 125 µL of Glutathione Sepharose 4B (Amersham Biosciences AB) were used for each ml of extract. Purification was performed following manufacturer's instruction, leaving the proteins linked to the resin that was soaked at 4 °C overnight, in a solution of 3% BSA (w/v) in PBS to achieve blocking.

Affinity chromatography

Mouse brain (from Black 6, C57BL/6J strains) was washed in PBS 1X and lysed in 100 µL of lysis buffer for each 100 µg of tissue. Lysis buffer was composed of: NaCl 150 mM; Tris-HCl pH 7.5 25 mM; DTT (in AcONa 10 mM pH 5.2) 2 mM; EDTA pH 7.5 2 mM; protease inhibitor mix for mammalian tissues from Sigma (AEBSF 104 mM, bestatin 4 mM, E-64 1.4 mM, leupeptin 2 mM, aprotinin 80 µM, pepstatin-A 1.5 mM); Triton X-100 1% (v/v); SDS 0.1% (w/v); sodium deoxycholate 1% (w/v). Samples were incubated for 45 min at 4 °C under constant agitation, then centrifuged and supernatants were diluted (at least 1:4) with lysis buffer deprived of surfactants in order to reach concentrations of Triton X-100 0.25%; SDS 0.025%; sodium deoxycholate 0.25%. Extracts were incubated with GST-PDZ fusion proteins immobilized on Glutathione Sepharose 4B beads at 4 °C for 2 h; washed three times with lysis buffer, and the binding proteins were eluted with SDS sample buffer and subjected to SDS/PAGE. Bands were visualized by Comassie brilliant blue R 250 staining.
Lysates of transfected HEK 293T cells expressing FLAG-tagged proteins were obtained in JS lysis buffer (Hepes pH 7.5 50mM; NaCl 150mM; glycerol 1% (v/v); EGTA 5mM; Sodium orthovanadate 2mM; PMSF 1mM; protease inhibitors mix 1X Sigma) and incubated with GST recombinant proteins, as described above.

In-gel trypsin digestion, MALDI-TOF PMF MS and database search

In-gel tryptic digestion of the excised bands was performed following standard protocols [18, 19] with minor modifications. Briefly, excised bands were reduced with 10 mM dithiothreitol, alkylated with 55 mM iodoacetamide and overnight digested with 12.5 ng/µL trypsin. Peptides were then extracted and directly loaded on the MALDI target.
The tryptic digest was mixed in a 1:1 ratio (v/v) with the matrix solution on the MALDI target according to the dried droplet method. The matrix solution consisted in a saturated solution of recrystallized α-cyano-4-hydroxy-*trans*-cinnamic acid (CHCA) in 50% (v/v) acetonitrile/0.1% trifluoroacetic acid. The tryptic digests where desalted and concentrated when needed, before sample loading on the target.
Spectra were acquired on a Voyager DE-STR Biospectrometry Workstation from Applied Biosystems/MDS Sciex; 337 nm UV laser, positive ion reflector mode, no fewer than 400 shots per spectra were accumulated, accelerating voltage 20˙000 V, grid voltage 64% of the accelerating voltage, delay time 200 ns, mass range 750-4000 Da, low mass gate 700 Da. The instrument was equipped with Voyager Control Panel 5.10 for instrument control and Data Explorer 4.0.0.0 for spectra analysis (calibration and peak detection). Spectra were internally calibrated on two signals: one trypsin autolysis peak and a matrix cluster adduct. Manually validated monoisotopic masses where then subjected to database analysis via the Mascot search program [20, 21] (in-house Mascot Server 2.1.04 from Matrix Science). The interrogated databases were the latest available NCBInr database (National Center for Biotechnology Information non-redundant protein database, 6655203 sequences at the moment of analysis) and UniRef100 database (UniProt Reference Clusters [22], version 13.5, 6133773 sequences at the moment of analysis). Search parameters were as follows: no initial taxonomic restriction, one missed cleavage was allowed for trypsin specificity, carbamidomethylation of cysteine was set as fixed modification while methionine oxidation was set as variable modification, mass tolerance for monoisotopic data was set to 50 ppm.

Cell culture and transient transfection

HEK 293T cells were grown at 37 °C with 5% CO_2 in D-MEM (Dulbecco's Modified Eagle Media) supplemented with GlutaMAX (Invitrogen), foetal bovine serum (FBS) 10% and Pen/Strep antibiotics. HN9.10e mouse neuroblastoma cells (kindly donated by Dr. L. Colombaioni, CNR, Pisa, Italy) were cultured in the same conditions. PC12 rat pheochromocytoma cells were generally cultured in collagen coated dishes at 37 °C in RPMI medium supplemented with 5% fetal bovine serum, 10% horse serum,

25 U/ml penicillin, and 25 µg/ml streptomycin in a humidified atmosphere containing 5% CO_2. Neuronal phenotype was induced by 72 h incubation with 100 ng/ml NGF (Alomone labs, Jerusalem, Israel).
Cells (50-70% confluence) were transiently transfected with Lipofectamine 2000 (LF2000® from Invitrogen) reagent, following manufacturer's instructions and analysed 24 or 48 h post-transfection.

Co-immunoprecipitation and Western blotting
HEK 293T cells were co-transfected with the appropriate expression vectors and lysed in JS buffer (see affinity chromatography). Co-immunoprecipitation was conducted according to standard procedure: 1 mg of cytosolic protein extracts were diluted with lysis buffer deprived of Triton X-100 to 0.25% (final conc.), loaded over anti-FLAG-M2 affinity resin (Sigma-Aldrich) and incubated o/n at 4 °C and subjected to 10% acrylamide or 12% acrylamide SDS/PAGE. Proteins were electroblotted on PVDF membranes using Semidry system (Amersham Biosciences). The blot was probed with the indicated antibodies using an ECL® Western blotting kit, according to the manufacturer's instructions (Pierce).

Cell fluorescence microscopy and image analysis
Fluorescence images were obtained using a conventional fluorescence microscope (Nikon eclipse E600) connected with a digital camera (Photometrix CoolSnap, Roper Scientific USA) with a 100X oil immersion objective lens. Confocal images were acquired by a Leica TCS SP2 inverted confocal microscope (Leica Microsystems AG, Wetzlar, Germany) equipped with an Ar laser for excitation at 488 nm. Images were pseudocolored and merged using Adobe Photoshop version CS2 (9.0.2). For immunocytochemical experiments, transfected HEK 293T, HeLa and HN9.10e cells were fixed in 4% paraformaldehyde in phosphate-buffered saline (PBS) for 20 min at room temperature, washed with PBS, permeabilized with 0,1% (v/v) of Triton X-100 for 10 min, incubated with 1% BSA in PBS and labelled with specific antibodies. PC12 cells, NGF-induced, were fixed with 3.7% paraformaldehyde for 15 min at room temperature, washed with PBS, incubated with 50 mM NH_4Cl for 10 min, rinsed, permeabilized with blocking buffer (2% BSA, 0.25% porcine skin gelatin, 0.2% glycine, 15% fetal calf serum and 0.1% Triton X-100, in PBS) and labelled with specific antibodies. For live cells imaging, transfected HEK 293T cells were grown in glass bottom Petri dishes (WillCo-dishes GW St-3522) mounted in a thermostated chamber at 37 °C (Leica Microsystems) and viewed with a 40X 1.25 numerical aperture oil immersion objective (Leica Microsystems). The images were collected using low excitation power at the sample (10-20 µW) and monitoring the emission by means of acousto-optical beam splitter (AOBS) detection system of the confocal microscope. In order to label endocytic structures, different glass bottom Petri dishes containing transfected cells were incubated with different dyes: 1 mg/ml of neutral 70 kDa dextran TMR-conjugated at 37 °C for 30 minutes to label pinosomes, with 50 nM of Lysotracker dye (LysoTracker Red DND-99) for 5 minutes to label lysosomes and with 2 µg/ml of transferrin-rhodaminated to label recycling and sorting endosomes.

RESULTS

Purification of CIPP-PDZ interacting proteins from mouse brain.
In order to search for neuronal proteins interacting with CIPP, we decided to exploit its modular nature: CIPP is a 612-aminoacid protein containing four PDZ domains. We resolved CIPP in its components, the single PDZ domains, to purify specific binders from protein extracts of mouse total brain, where this short isoform of an apparent molecular weight of 60 kDa is preferentially expressed [5, 15].
Each PDZ domain of CIPP was isolated by PCR amplification from a full length cDNA clone (IMAGE n. 641366) and expressed in bacteria as glutathione S-transferase (GST) fusion. Recombinant proteins were immobilized on Glutathione Sepharose beads and used, in parallel to control GST, as bait to select

specific interactors from Triton X-100-solubilized mouse brain extract. Bound proteins were separated by mono-dimensional polyacrylamide gel electrophoresis in denaturing conditions (SDS-PAGE) and specific bands, stained with Comassie blue, were cut from the gel and subjected to mass spectrometry (MS) analysis via MALDI-TOF PMF. Taking into account the bands pulled-down by GST-PDZ and not by GST alone, specific interacting proteins were isolated with domains PDZ-1 and PDZ-2 (Fig. 1). In contrast, PDZ-3 and PDZ-4 didn't select any noticeable protein (data not shown). We assumed that some membrane receptors, previously identified as CIPP partners using different approaches [5, 12], were not present or were undetectable among the bands we selected for further MS analysis; indeed, during our purification procedure the majority of transmembrane neural proteins were discarded and we concentrated our analysis on the central part of the gels, where differences between samples and controls were more marked (Fig. 1 arrows).
Results of MS analysis are resumed in Table 1, where identified proteins with significant score values are listed.

> Insert Table 1

In all the excised bands it was possible to unambiguously identify one or more proteins. Absence of the corresponding proteins, in bands excised from the control lanes, was assessed to avoid selecting contaminants. The high number of bands pulled down by a single PDZ domain could be caused by the purification of multiprotein complexes, including direct and indirect PDZ ligands. Indeed, several of the identified proteins have been described in common signal transduction pathways, resulting often implicated in cytoskeletal dynamics. Both alpha and beta subunits of Calcium/calmodulin-dependent protein kinase type II (CaMKII), together with actin and tubulin were among the major bands. CaMKII is a serine/threonine kinase involved in various forms of neuronal plasticity that targets F-actin and associated proteins to dendritic spines [23, 24]. Other interactors related to actin were serine/threonine-protein phosphatase 2B catalytic subunit alpha isoform (CALNA), which regulates neuronal actin cytoskeletal dynamics via calcium-dependent calmodulin stimulation, and insulin receptor tyrosine kinase substrate protein p53 (IRSp53-S, short isoform), a multidomain adaptor protein involved in the formation of membrane protrusions [17]. Furthermore, two tubulin-associated proteins were identified: 2',3'-cyclic nucleotide-3'-phosphodiesterase (CNP), a membrane-associated phosphodiesterase that regulates cytoplasmic microtubule distribution [25], and guanine deaminase (Cypin), an enzyme that regulates dendrite morphology, promoting microtubule assembly and directly binding to tubulin heterodimers [26, 27].

Analysis of CIPP-PDZ direct interactions

In order to distinguish those interactors directly binding to CIPP PDZ domains, we examined the sequences at the carboxy-terminus of each identified protein, searching for specific PDZ binding motifs. PDZ domains preferentially recognize and bind targets ending with a hydrophobic carboxy-terminal residue (in position 0) and a key residue (in position -2) that are critical for binding specificity and determinant for classifying PDZ ligands. Other upstream residues are also important for improving the binding efficiency, but mutations in the two crucial positions are usually sufficient to prevent the binding [28, 29]. In a previous study, using a peptide phage library containing nine random residues, we assessed the binding specificity of the PDZ domains of the human ortholog of CIPP: the protein INADL (afterwards named PATJ) [30]. As the first two PDZ of the mouse CIPP share high homology (97%) with the last two PDZ of the human isoform we used in our screening, it is possible to predict their binding preference. Both PDZ1 and PDZ2 of CIPP should prefer class I ligands (characterized by Serine or Threonine in position -2 and a hydrophobic residue at the extremity). This preference was directly confirmed in a more recent study, where the binding specificity of CIPP-PDZ was determined

by screening a combinatorial synthetic peptide library, containing five random residues [31]. Sequence inspection of the proteins identified by MS analysis revealed that three of the selected proteins share C-terminal PDZ binding motifs of class I (S or T in position -2). They are: Cypin ending with residues "$S_{-2}S_{-1}V_0$"; CNP ending with residues "$T_{-2}I_{-1}I_0$" and IRSp53 ending with "$S_{-2}T_{-1}V_0$". Therefore, these three proteins represent the most probable direct ligands, while the other identified interactors likely bind to CIPP PDZ domains in an indirect way or by contacting different regions.

To prove that the binding mode of CIPP to Cypin, CNP and IRSp53 was direct and specific, we isolated the corresponding cDNA by PCR amplification of the available Cypin and CNP IMAGE clones; at variance, we directly amplified IRSp53-S (the short isoform with the PDZ binding motif) by RT-PCR from mouse brain RNA, since a corresponding IMAGE clone was not available. We generated the corresponding FLAG-tagged constructs, transfected them in cultured HEK 293T cells and performed pull-down experiments using GST-PDZ-1 and GST-PDZ2 as baits (Fig. 2A). Results confirmed that Cypin binds to PDZ1, while both CNP and IRSp53 bind to PDZ2 domain.
Next we tested whether such interactions could also occur in living cells, using the full-length CIPP protein, containing the four PDZ domains. This was an important control, because PDZ domains may sometimes influence the folding of the adjacent domains, avoiding or enhancing specific binding to target ligands [32-34]. We fused full-length CIPP to green fluorescent GFP protein and analysed its binding potential by co-transfection with FLAG-tagged Cypin, FLAG-CNP or FLAG-IRSp53 and co-immunoprecipitation with anti-FLAG. The presence of GFP-CIPP, but not GFP alone in the immunoprecipitates revealed that the binding also occurs within intact cells (Fig. 2B).

CIPP has a cytosolic localization but it is redistributed in presence of IRSp53

The localization of GFP-CIPP and of its interacting proteins in transfected cells was examined by immunocitochemistry. Green fluorescence derived from GFP-CIPP expression was diffused through the cytoplasm of HEK 293T cells, with some perinuclear concentration (Fig. 3A). A similar distribution was observed for FLAG-Cypin, as revealed by immunostaining (Fig. 3B), while FLAG-CNP was mainly localised at membrane level, forming protruding structures and aggregates (Fig. 3C), as already described [25]. The formation of membrane protrusions such as filopodia and lamellipodia was even more pronounced after transfecting FLAG-IRSp53 (Fig. 3D). Indeed, such a property of IRSp53 has been confirmed in different types of transfected cells [17]. When a double transfection of CIPP with Cypin or with CNP was performed in HEK 293T cells, no significant change in their distribution was observed. Localization of Cypin could be entirely superimposed to GFP-CIPP, when both proteins were overexpressed in the cells (Fig. 3, panels E). On the other hand, only a fraction of GFP-CIPP was membrane-associated and co-localized with CNP, while its distribution remained largely diffused, not forming aggregates (Fig. 3, panels F). In contrast, when GFP-CIPP was co-expressed with FLAG-IRSp53, a marked reorganization of its localization was observed (Fig. 3, panels G). Both proteins clusterize in punctate structures dispersed in the cytosol and in membrane protrusions, particularly at the filopodia tips (Fig. 3, panels H).
Puncta formation was a peculiar effect of IRSp53/CIPP co-expression and it was not due to over-expression, since CIPP-redistribution was not observed, after co-transfection with the other FLAG constructs. To exclude the possibility that such effect was related to the HEK 293T model system, we investigated the ability of IRSp53 to induce CIPP puncta formation also in neuronal cell types: namely, rat PC12 induced to a neuronal phenotype by NGF and murine neuroblastoma HN9.10e, a cell line that spontaneously exhibits morphological, cytoskeletal and electrophysiological features typical of its neuronal parents [35]. GFP-CIPP expression in these cells was diffused, but following IRSp53 co-transfection, the formation of punctate structures was always detectable (representative cells in Fig. 4, panels C and F).

In order to establish if the PDZ-mediated binding of CIPP to IRSp53 was essential for puncta formation, to disrupt the PDZ binding motif we substituted the four residues at the IRSp53 carboxyl-terminus "$V_{-3}S_{-2}T_{-1}V_{-0}$" with residues "$A_{-3}A_{-2}P_{-1}T_{0}$". Co-transfection of GFP-CIPP with this substitution mutant (C-mut-IRSp53) did not induce puncta formation, proving the importance of the PDZ-binding motif (Fig. 5, panels A). As expected, the typical IRSp53 property of inducing membrane protrusions, as filopodia and lamellipodia, was not impaired (arrowhead). In fact, the main domain involved in such activity is the N-terminal IMD (IRSp53-MIM Domain), also named I-BAR domain (Inverse-Bin-Amphiphysins-Rvs) for its ability of bending membranes with a mechanism opposite to classical BAR domain [36, 37]. Also involved is the partial CRIB domain, binding to small GTPase Cdc42 [38-42] with the coupled contribute of the SH3 domain and associated proteins, as suggested by recent work [17, 36]. A deletion mutant of IRSp53, lacking the IMD and the partial CRIB domains (N-mut-IRSp53), was unable to induce filopodia formation in HEK 293T cells; on the other hand, when co-transfected with GFP- CIPP, it exhibited extensive co-localization and formation of large cytoplasmic puncta (Fig. 5, panels B). These observations were confirmed by co-immunoprecipitation assays: extracts of HEK 293T cells transfected with GFP-CIPP and N or C mutants of IRSp53 were immunoprecipitated with anti-FLAG and tested by immunoblot with anti-GFP. As shown in Fig. 5C, the interaction of C-mut-IRSp53 with GFP-CIPP was precluded, while N-mut-IRSp53 retained the ability to co-immunoprecipitate GFP-CIPP (Fig. 5D).

Since CIPP modular structure should make the protein able to simultaneously connect multiple binders, we hypothesized that the puncta caused by IRSp53/CIPP interaction could include other proteins binding to distinct PDZ domains. IRSp53 binds to PDZ2. In particular, since Cypin binds to PDZ1 and maintains its diffused localization also in presence of CIPP, it was considered a good candidate for such analysis. On the contrary, CNP was not considered suitable, because it spontaneously forms aggregates and clusters, also when it is transiently expressed alone (Fig. 3C). To explore the possibility that Cypin could be incorporated in the punctate structures, we used a HA-tagged-Cypin construct. This construct was first co-transfected either with GFP-CIPP or with FLAG-IRSp53 alone, to control the absence of puncta formation (Fig. 6, panels A and B). In contrast, co-transfection of the three constructs together, followed by HA-specific immunostaining (red), revealed that also Cypin was encompassed in the puncta generated by IRSp53-CIPP interaction (green staining) (Fig. 6, panels C).

Analysis of the puncta nature

The punctate structures observed following transient co-expression of FLAG-IRSp53 with GFP-CIPP have different shape and size (approximately ranging from 50 nm to 3 μm). To gain insight into the identity of these structures, we examined a potential relationship to cellular vesicles involved in the main endocytic pathways. Such hypothesis was strengthened by the frequent association of actin effectors and cytoskeletal remodeling with vesicles recycling; for instance, a synergistic effect of IRSp53 with Rac1, Wave2, and Rah on membrane ruffling and on subsequent macropinosomes formation has been reported [43]. To discriminate among different types of cytoplasmic vesicles, we performed co-localization studies in living cells using well-known endocytic biomarkers.

HEK 293T cells were co-transfected with CIPP-GFP and FLAG-IRSp53 and *in vivo* labelled for dextran (to identify pinosomes in macropinocytosis), for transferrin (a well recognized marker of early-sorting and recycling endosomes) and for lysotracker (labelling late endosomes and lysosomes). Co-localization of labelled red vesicles with green GFP-CIPP puncta was rarely observed (Fig. 7, panel 1). Similar results were obtained in fixed HeLa cells, expressing CIPP-GFP and FLAG-IRSp53 that were stained with specific antibodies against common vacuolar structures (Fig. 7, panel 2) and against membrane markers as EGFR (data not shown). Punctate patterns (green) never co-stained with the

analysed markers. They seem to be related neither to membranes, nor to endocytic compartments, as they failed to co-localize with EEA1, clathrin heavy chain, and LAMP2 endosomal, which highlight clathrin vesicles and lysosomal markers. We also tested a potential association to the Golgi complex, using an anti-giantin antibody, but no co-staining was observed.
Therefore we conclude that cytoplasmic puncta are not related to cytoplasmic vesicles. They rather appear to correspond to intracellular structures made of large protein assemblies, where CIPP is trained by IRSp53.

DISCUSSION

Modular proteins, like multi-PDZ CIPP, are frequently involved in organizing molecular complexes with structural or functional roles in signal transduction. Unravelling the components of the networks mediated by such multivalent binding proteins is essential for understanding how the systems work.
Neuronal CIPP is composed by four PDZ domains, each probably involved in a specific binding. Although several membrane receptors and channels have been proposed as CIPP-PDZ binders, there has been no report indicating the corresponding cytosolic partners; therefore, the mechanisms by which CIPP transduces the signals from such receptors into the cells are poorly understood [5, 12-14].
In this study we present a list of potential CIPP interacting proteins, selected from mouse brain extracts by GST-PDZ mediated affinity chromatography. The majority of the bands, identified by mass spectrometry analysis, represent cytosolic proteins, including enzymes and effectors associated with synaptic structures formation and receptor-linked plasticity. These findings can be useful to infer the binding potential of CIPP protein, although further studies on individual proteins are necessary to demonstrate their participation in a common network. For instance, the kinase CaMKII and the phosphatase CALNA - both involved in signal pathways regulated by the level of Ca^{2+} influx through the NMDA-type glutamate receptors [44, 45] - were identified as the most abundant specific bands, but they lack a C-terminal PDZ binding motif that would prove a direct binding to CIPP. Actually, unusual binding to an internal peptide sequence of CaMKII, through the second PDZ of MUPP1 (a paralog of CIPP/INADL) has been already reported [46]. Thus, such binding modality could also be exploited by CIPP-PDZ.
In contrast, other proteins are easily recognizable as direct binders by simple inspection of their carboxy-terminus: CNP, Cypin and IRSp53 do not share homologous C-terminal sequences, but all have class-I PDZ binding motifs, which have been predicted as CIPP preferred ligands by combinatorial studies [30, 31]. There is a thread linking these proteins that is their involvement in cytoskeletal remodeling, associated to tubulin and actin dynamics. We have analysed in detail the interaction between CIPP and IRSp53, a typical regulator of membrane and actin dynamics. IRSp53 was originally identified as a substrate for insulin receptor tyrosine kinase or as the brain-specific angiogenesis inhibitor 1-associated protein 2 (BAIAP2) [47, 48]. Several variants, differing in length and sequence have been described; in the brain, a long IRSp53-(L) and a short IRSp53-(S) isoforms are mainly expressed [17]. The crucial role of IRSp53, as organizer of multiprotein complexes, has been clarified by characterizing its distinct binding domains, which synergistically act to promote actin dynamics and filopodia and lamellipodia protrusion activities [17, 36]. They are the IMD (I-BAR) domain at the amino-terminus, which promotes membrane bending and protrusions [36, 37, 49]; a partial CRIB motif (Cdc42/Rac interactive binding), showing an affinity for small GTPases that is higher for Cdc42 than for Rac1 [36, 38, 39]; an SH3 domain, which has been shown to mediate the interaction with a variety of signaling proteins: Wave2, Mena, Eps8 proteins; finally, at the carboxyl terminus, a WH2 like domain in L variant or a PDZ binding motif in S variant, which further enlarges the spectrum of interactions to multiple PDZ proteins, as PSD95, MALS, Shank1 ([17] and references therein). Actually, in our affinity selection with the second PDZ of CIPP we purified the short variant

(S), ending with the class-I PDZ binding motif and we found that this motif is essential to provoke the clustering of IRSp53 and CIPP in punctate structures of various size and shape, when both proteins were ectopically expressed in mammalian cultured cells of epithelial or neuronal derivation. Such structures do not form when CIPP is expressed with the other ligands we identified, CNP or Cypin. A potential correlation of puncta with endocytotic vesicles was suggested by a previously described association of IRSp53 with macropinosomes formation [43] or by the observation that in epithelial cells a longer CIPP isoform (PATJ) can be delivered to plasma membrane in vesicles and recycled into endosomes, together with other components of tight junction complexes [50]. Therefore, in order to clarify if the large puncta observed in our system were effectively related to membrane trafficking, we performed a detailed analysis with a set of vesicle markers. The immunostaining results plainly disclaimed this hypothesis, underlying the differences between the isoforms. In effect, presence of an aminoterminal unique L27/MRE domain in the long isoform results essential for association to PALS and participation in the establishment of the tight junctions, linking ZO-3 and claudin-1 [10, 11, 51]. The L27/MRE domain is absent in the short isoform CIPP, which contains only four PDZ domains and therefore, probably, has a different role in neuronal cells.

Our findings, combined with the literature reports, shed light on the possible multiprotein complexes that CIPP-PDZ domains contribute to assembly. For example, many evidences point out an involvement of CIPP in NMDA receptor mediated transduction. Previous studies have demonstrated that the NR2A or NR2D subunits of the NMDA receptor specifically interact with the third PDZ of CIPP [5]. Here we have shown that IRSp53 directly binds to the second CIPP-PDZ and that Cypin, a protein that promotes microtubule assembly by interacting with tubulin heterodimers, directly binds to the first CIPP-PDZ.

Moreover, IRSp53 is known to be rapidly accumulated at neuronal postsynaptic sites, following glutamate or NMDA stimulation, where it facilitates cytoskeletal reorganization and neurite outgrowth [16, 38]. Mechanisms coordinating actin and microtubule dynamics in membrane trafficking and filament processing are object of multiple current studies. The association of small GTPases, such as Cdc42 and Rac with IRSp53 and of RhoA with Cypin has been extensively proved [27, 38-42, 52]. Interestingly, combined regulation of small GTPases by NMDA receptor activation has been described: increase of Cdc42 and Rac activity and decrease of RhoA activity is required for the promotion of dendritic growth of *Xenopus* optic tectal neurons [53, 54]. The hypothesis that CIPP-PDZ could mediate the association of Cypin and IRSp53 with NMDA receptors is attractive.

Actually, diverse PDZ proteins are known to bind to NMDA subunit C-termini, firstly the prototypical PDZ protein PSD-95, which is responsible of neural transmission and excitotoxicity [1]. Nevertheless, it has been recently proved, using a proteomic approach, that different affinities for the same NMDA receptor carboxy-terminal ligand can modulate the binding of one or another potential interacting PDZ protein, activating different signaling pathways [55].

It will be important to extend our study, confirming the co-participation of the different components in endogenous CIPP-mediated networks. However, all information we obtained from the MS analysis and the ectopic expression of CIPP with its interactors in cultured cells, indicate that they converge in a common pathway, where CIPP-PDZ domains could be the bridge between actin and tubulin associated proteins.

AKNOWLEDGEMENTS

We especially thank Dr.F. Cremisi and Prof. G. Barsacchi for careful reading of the manuscript and Prof. F. Beltram for support and hospitality at the Confocal Microscopy Facility (NEST, SNS, Pisa). We are grateful to M. Fabbri and G. De Matienzo for excellent technical support. E. Alpi was recipient of a mobility fellowship from the Italian Proteomic Association (formerly Italian section of Human

Proteome Organization) during his PhD program at the Department of Chemistry and Industrial Chemistry, University of Pisa. This work was supported by Centro di Eccellenza AmbiSEN-Pisa; by MIUR (PRIN 2006054104_002) and by Contributo Ministero Affari Esteri Cooperazione Italia-Cina R.P. (NFNS 30370453).

REFERENCES

1 Sheng, M. and Sala, C. (2001) PDZ domains and the organization of supramolecular complexes. Annu Rev Neurosci. **24**, 1-29

2 Nourry, C., Grant, S. G. and Borg, J. P. (2003) PDZ domain proteins: plug and play! Sci STKE. **2003**, RE7

3 van Ham, M. and Hendriks, W. (2003) PDZ domains-glue and guide. Mol Biol Rep. **30**, 69-82

4 Kim, E. and Sheng, M. (2004) PDZ domain proteins of synapses. Nat Rev Neurosci. **5**, 771-781

5 Kurschner, C., Mermelstein, P. G., Holden, W. T. and Surmeier, D. J. (1998) CIPP, a novel multivalent PDZ domain protein, selectively interacts with Kir4.0 family members, NMDA receptor subunits, neurexins, and neuroligins. Mol Cell Neurosci. **11**, 161-172

6 Carninci, P., Kasukawa, T., Katayama, S., Gough, J., Frith, M. C., Maeda, N., Oyama, R., Ravasi, T., Lenhard, B., Wells, C., Kodzius, R., Shimokawa, K., Bajic, V. B., Brenner, S. E., Batalov, S., Forrest, A. R., Zavolan, M., Davis, M. J., Wilming, L. G., Aidinis, V., Allen, J. E., Ambesi-Impiombato, A., Apweiler, R., Aturaliya, R. N., Bailey, T. L., Bansal, M., Baxter, L., Beisel, K. W., Bersano, T., Bono, H., Chalk, A. M., Chiu, K. P., Choudhary, V., Christoffels, A., Clutterbuck, D. R., Crowe, M. L., Dalla, E., Dalrymple, B. P., de Bono, B., Della Gatta, G., di Bernardo, D., Down, T., Engstrom, P., Fagiolini, M., Faulkner, G., Fletcher, C. F., Fukushima, T., Furuno, M., Futaki, S., Gariboldi, M., Georgii-Hemming, P., Gingeras, T. R., Gojobori, T., Green, R. E., Gustincich, S., Harbers, M., Hayashi, Y., Hensch, T. K., Hirokawa, N., Hill, D., Huminiecki, L., Iacono, M., Ikeo, K., Iwama, A., Ishikawa, T., Jakt, M., Kanapin, A., Katoh, M., Kawasawa, Y., Kelso, J., Kitamura, H., Kitano, H., Kollias, G., Krishnan, S. P., Kruger, A., Kummerfeld, S. K., Kurochkin, I. V., Lareau, L. F., Lazarevic, D., Lipovich, L., Liu, J., Liuni, S., McWilliam, S., Madan Babu, M., Madera, M., Marchionni, L., Matsuda, H., Matsuzawa, S., Miki, H., Mignone, F., Miyake, S., Morris, K., Mottagui-Tabar, S., Mulder, N., Nakano, N., Nakauchi, H., Ng, P., Nilsson, R., Nishiguchi, S., Nishikawa, S., Nori, F., Ohara, O., Okazaki, Y., Orlando, V., Pang, K. C., Pavan, W. J., Pavesi, G., Pesole, G., Petrovsky, N., Piazza, S., Reed, J., Reid, J. F., Ring, B. Z., Ringwald, M., Rost, B., Ruan, Y., Salzberg, S. L., Sandelin, A., Schneider, C., Schonbach, C., Sekiguchi, K., Semple, C. A., Seno, S., Sessa, L., Sheng, Y., Shibata, Y., Shimada, H., Shimada, K., Silva, D., Sinclair, B., Sperling, S., Stupka, E., Sugiura, K., Sultana, R., Takenaka, Y., Taki, K., Tammoja, K., Tan, S. L., Tang, S., Taylor, M. S., Tegner, J., Teichmann, S. A., Ueda, H. R., van Nimwegen, E., Verardo, R., Wei, C. L., Yagi, K., Yamanishi, H., Zabarovsky, E., Zhu, S., Zimmer, A., Hide, W., Bult, C., Grimmond, S. M., Teasdale, R. D., Liu, E. T., Brusic, V., Quackenbush, J., Wahlestedt, C., Mattick, J. S., Hume, D. A., Kai, C., Sasaki, D., Tomaru, Y., Fukuda, S., Kanamori-Katayama, M., Suzuki, M., Aoki, J., Arakawa, T., Iida, J., Imamura, K., Itoh, M., Kato, T., Kawaji, H., Kawagashira, N., Kawashima, T., Kojima, M., Kondo, S., Konno, H., Nakano, K., Ninomiya, N., Nishio, T., Okada, M., Plessy, C., Shibata, K., Shiraki, T., Suzuki, S., Tagami, M., Waki, K., Watahiki, A., Okamura-Oho, Y., Suzuki, H., Kawai, J. and Hayashizaki, Y. (2005) The transcriptional landscape of the mammalian genome. Science. **309**, 1559-1563

7 Philipp, S. and Flockerzi, V. (1997) Molecular characterization of a novel human PDZ domain protein with homology to INAD from Drosophila melanogaster. FEBS Lett. **413**, 243-248

8 Lemmers, C., Medina, E., Delgrossi, M. H., Michel, D., Arsanto, J. P. and Le Bivic, A. (2002) hINADl/PATJ, a homolog of discs lost, interacts with crumbs and localizes to tight junctions in human epithelial cells. J Biol Chem. **277**, 25408-25415

9 Bhat, M. A., Izaddoost, S., Lu, Y., Cho, K. O., Choi, K. W. and Bellen, H. J. (1999) Discs Lost, a novel multi-PDZ domain protein, establishes and maintains epithelial polarity. Cell. **96**, 833-845

10 Roh, M. H., Makarova, O., Liu, C. J., Shin, K., Lee, S., Laurinec, S., Goyal, M., Wiggins, R. and Margolis, B. (2002) The Maguk protein, Pals1, functions as an adapter, linking mammalian homologues of Crumbs and Discs Lost. J Cell Biol. **157**, 161-172

11 Roh, M. H. and Margolis, B. (2003) Composition and function of PDZ protein complexes during cell polarization. Am J Physiol Renal Physiol. **285**, F377-387

12 Anzai, N., Deval, E., Schaefer, L., Friend, V., Lazdunski, M. and Lingueglia, E. (2002) The multivalent PDZ domain-containing protein CIPP is a partner of acid-sensing ion channel 3 in sensory neurons. J Biol Chem. **277**, 16655-16661

13 Becamel, C., Gavarini, S., Chanrion, B., Alonso, G., Galeotti, N., Dumuis, A., Bockaert, J. and Marin, P. (2004) The serotonin 5-HT2A and 5-HT2C receptors interact with specific sets of PDZ proteins. J Biol Chem. **279**, 20257-20266

14 Joubert, L., Hanson, B., Barthet, G., Sebben, M., Claeysen, S., Hong, W., Marin, P., Dumuis, A. and Bockaert, J. (2004) New sorting nexin (SNX27) and NHERF specifically interact with the 5-HT4a receptor splice variant: roles in receptor targeting. J Cell Sci. **117**, 5367-5379

15 Chanrion, B., Mannoury la Cour, C., Bertaso, F., Lerner-Natoli, M., Freissmuth, M., Millan, M. J., Bockaert, J. and Marin, P. (2007) Physical interaction between the serotonin transporter and neuronal nitric oxide synthase underlies reciprocal modulation of their activity. Proc Natl Acad Sci U S A. **104**, 8119-8124

16 Hori, K., Yasuda, H., Konno, D., Maruoka, H., Tsumoto, T. and Sobue, K. (2005) NMDA receptor-dependent synaptic translocation of insulin receptor substrate p53 via protein kinase C signaling. J Neurosci. **25**, 2670-2681

17 Scita, G., Confalonieri, S., Lappalainen, P. and Suetsugu, S. (2008) IRSp53: crossing the road of membrane and actin dynamics in the formation of membrane protrusions. Trends Cell Biol. **18**, 52-60

18 Shevchenko, A., Wilm, M., Vorm, O. and Mann, M. (1996) Mass spectrometric sequencing of proteins silver-stained polyacrylamide gels. Anal Chem. **68**, 850-858

19 Shevchenko, A., Tomas, H., Havlis, J., Olsen, J. V. and Mann, M. (2006) In-gel digestion for mass spectrometric characterization of proteins and proteomes. Nat Protoc. **1**, 2856-2860

20 Pappin, D. J., Hojrup, P. and Bleasby, A. J. (1993) Rapid identification of proteins by peptide-mass fingerprinting. Curr Biol. **3**, 327-332

21 Perkins, D. N., Pappin, D. J., Creasy, D. M. and Cottrell, J. S. (1999) Probability-based protein identification by searching sequence databases using mass spectrometry data. Electrophoresis. **20**, 3551-3567

22 Suzek, B. E., Huang, H., McGarvey, P., Mazumder, R. and Wu, C. H. (2007) UniRef: comprehensive and non-redundant UniProt reference clusters. Bioinformatics. **23**, 1282-1288

23 Shen, K., Teruel, M. N., Subramanian, K. and Meyer, T. (1998) CaMKIIbeta functions as an F-actin targeting module that localizes CaMKIIalpha/beta heterooligomers to dendritic spines. Neuron. **21**, 593-606

24 Lisman, J., Schulman, H. and Cline, H. (2002) The molecular basis of CaMKII function in synaptic and behavioural memory. Nat Rev Neurosci. **3**, 175-190

25 Bifulco, M., Laezza, C., Stingo, S. and Wolff, J. (2002) 2',3'-Cyclic nucleotide 3'-phosphodiesterase: a membrane-bound, microtubule-associated protein and membrane anchor for tubulin. Proc Natl Acad Sci U S A. **99**, 1807-1812

26 Akum, B. F., Chen, M., Gunderson, S. I., Riefler, G. M., Scerri-Hansen, M. M. and Firestein, B. L. (2004) Cypin regulates dendrite patterning in hippocampal neurons by promoting microtubule assembly. Nat Neurosci. **7**, 145-152

27 Chen, H. and Firestein, B. L. (2007) RhoA regulates dendrite branching in hippocampal neurons by decreasing cypin protein levels. J Neurosci. **27**, 8378-8386

28 Doyle, D. A., Lee, A., Lewis, J., Kim, E., Sheng, M. and MacKinnon, R. (1996) Crystal structures of a complexed and peptide-free membrane protein-binding domain: molecular basis of peptide recognition by PDZ. Cell. **85**, 1067-1076

29 Songyang, Z., Fanning, A. S., Fu, C., Xu, J., Marfatia, S. M., Chishti, A. H., Crompton, A., Chan, A. C., Anderson, J. M. and Cantley, L. C. (1997) Recognition of unique carboxyl-terminal motifs by distinct PDZ domains. Science. **275**, 73-77

30 Vaccaro, P., Brannetti, B., Montecchi-Palazzi, L., Philipp, S., Helmer Citterich, M., Cesareni, G. and Dente, L. (2001) Distinct binding specificity of the multiple PDZ domains of INADL, a human protein with homology to INAD from Drosophila melanogaster. J Biol Chem. **276**, 42122-42130

31 Joo, S. H. and Pei, D. (2008) Synthesis and screening of support-bound combinatorial peptide libraries with free C-termini: determination of the sequence specificity of PDZ domains. Biochemistry. **47**, 3061-3072

32 Lockless, S. W. and Ranganathan, R. (1999) Evolutionarily conserved pathways of energetic connectivity in protein families. Science. **286**, 295-299

33 Grootjans, J. J., Reekmans, G., Ceulemans, H. and David, G. (2000) Syntenin-syndecan binding requires syndecan-synteny and the co-operation of both PDZ domains of syntenin. J Biol Chem. **275**, 19933-19941

34 van den Berk, L. C., Landi, E., Walma, T., Vuister, G. W., Dente, L. and Hendriks, W. J. (2007) An allosteric intramolecular PDZ-PDZ interaction modulates PTP-BL PDZ2 binding specificity. Biochemistry. **46**, 13629-13637

35 Lee, H. J., Hammond, D. N., Large, T. H., Roback, J. D., Sim, J. A., Brown, D. A., Otten, U. H. and Wainer, B. H. (1990) Neuronal properties and trophic activities of immortalized hippocampal cells from embryonic and young adult mice. J Neurosci. **10**, 1779-1787

36 Lim, K. B., Bu, W., Goh, W. I., Koh, E., Ong, S. H., Pawson, T., Sudhaharan, T. and Ahmed, S. (2008) The Cdc42 effector IRSp53 generates filopodia by coupling membrane protrusion with actin dynamics. J Biol Chem. **283**, 20454-20472

37 Mattila, P. K., Pykalainen, A., Saarikangas, J., Paavilainen, V. O., Vihinen, H., Jokitalo, E. and Lappalainen, P. (2007) Missing-in-metastasis and IRSp53 deform PI(4,5)P2-rich membranes by an inverse BAR domain-like mechanism. J Cell Biol. **176**, 953-964

38 Govind, S., Kozma, R., Monfries, C., Lim, L. and Ahmed, S. (2001) Cdc42Hs facilitates cytoskeletal reorganization and neurite outgrowth by localizing the 58-kD insulin receptor substrate to filamentous actin. J Cell Biol. **152**, 579-594

39 Krugmann, S., Jordens, I., Gevaert, K., Driessens, M., Vandekerckhove, J. and Hall, A. (2001) Cdc42 induces filopodia by promoting the formation of an IRSp53:Mena complex. Curr Biol. **11**, 1645-1655

40 Nakagawa, H., Miki, H., Nozumi, M., Takenawa, T., Miyamoto, S., Wehland, J. and Small, J. V. (2003) IRSp53 is colocalised with WAVE2 at the tips of protruding lamellipodia and filopodia independently of Mena. J Cell Sci. **116**, 2577-2583

41 Yamagishi, A., Masuda, M., Ohki, T., Onishi, H. and Mochizuki, N. (2004) A novel actin bundling/filopodium-forming domain conserved in insulin receptor tyrosine kinase substrate p53 and missing in metastasis protein. J Biol Chem. **279**, 14929-14936

42 Millard, T. H., Bompard, G., Heung, M. Y., Dafforn, T. R., Scott, D. J., Machesky, L. M. and Futterer, K. (2005) Structural basis of filopodia formation induced by the IRSp53/MIM homology domain of human IRSp53. EMBO J. **24**, 240-250

43 Sun, P., Yamamoto, H., Suetsugu, S., Miki, H., Takenawa, T. and Endo, T. (2003) Small GTPase Rah/Rab34 is associated with membrane ruffles and macropinosomes and promotes macropinosome formation. J Biol Chem. **278**, 4063-4071

44 Leonard, A. S., Bayer, K. U., Merrill, M. A., Lim, I. A., Shea, M. A., Schulman, H. and Hell, J. W. (2002) Regulation of calcium/calmodulin-dependent protein kinase II docking to N-methyl-D-aspartate receptors by calcium/calmodulin and alpha-actinin. J Biol Chem. **277**, 48441-48448

45 Choi, J. Y., Beaman-Hall, C. M. and Vallano, M. L. (2004) Granule neurons in cerebellum express distinct splice variants of the inositol trisphosphate receptor that are modulated by calcium. Am J Physiol Cell Physiol. **287**, C971-980

46 Krapivinsky, G., Medina, I., Krapivinsky, L., Gapon, S. and Clapham, D. E. (2004) SynGAP-MUPP1-CaMKII synaptic complexes regulate p38 MAP kinase activity and NMDA receptor-dependent synaptic AMPA receptor potentiation. Neuron. **43**, 563-574

47 Abbott, M. A., Wells, D. G. and Fallon, J. R. (1999) The insulin receptor tyrosine kinase substrate p58/53 and the insulin receptor are components of CNS synapses. J Neurosci. **19**, 7300-7308

48 Oda, K., Shiratsuchi, T., Nishimori, H., Inazawa, J., Yoshikawa, H., Taketani, Y., Nakamura, Y. and Tokino, T. (1999) Identification of BAIAP2 (BAI-associated protein 2), a novel human homologue of hamster IRSp53, whose SH3 domain interacts with the cytoplasmic domain of BAI1. Cytogenet Cell Genet. **84**, 75-82

49 Suetsugu, S., Murayama, K., Sakamoto, A., Hanawa-Suetsugu, K., Seto, A., Oikawa, T., Mishima, C., Shirouzu, M., Takenawa, T. and Yokoyama, S. (2006) The RAC binding domain/IRSp53-MIM homology domain of IRSp53 induces RAC-dependent membrane deformation. J Biol Chem. **281**, 35347-35358

50 Wells, C. D., Fawcett, J. P., Traweger, A., Yamanaka, Y., Goudreault, M., Elder, K., Kulkarni, S., Gish, G., Virag, C., Lim, C., Colwill, K., Starostine, A., Metalnikov, P. and Pawson, T. (2006) A Rich1/Amot complex regulates the Cdc42 GTPase and apical-polarity proteins in epithelial cells. Cell. **125**, 535-548

51 Schneeberger, E. E. and Lynch, R. D. (2004) The tight junction: a multifunctional complex. Am J Physiol Cell Physiol. **286**, C1213-1228

52 Disanza, A., Mantoani, S., Hertzog, M., Gerboth, S., Frittoli, E., Steffen, A., Berhoerster, K., Kreienkamp, H. J., Milanesi, F., Di Fiore, P. P., Ciliberto, A., Stradal, T. E. and Scita, G. (2006) Regulation of cell shape by Cdc42 is mediated by the synergic actin-bundling activity of the Eps8-IRSp53 complex. Nat Cell Biol. **8**, 1337-1347

53 Li, Z., Van Aelst, L. and Cline, H. T. (2000) Rho GTPases regulate distinct aspects of dendritic arbor growth in Xenopus central neurons in vivo. Nat Neurosci. **3**, 217-225

54 Li, Z., Aizenman, C. D. and Cline, H. T. (2002) Regulation of rho GTPases by crosstalk and neuronal activity in vivo. Neuron. **33**, 741-750

55 Cui, H., Hayashi, A., Sun, H. S., Belmares, M. P., Cobey, C., Phan, T., Schweizer, J., Salter, M. W., Wang, Y. T., Tasker, R. A., Garman, D., Rabinowitz, J., Lu, P. S. and Tymianski, M. (2007) PDZ protein interactions underlying NMDA receptor-mediated excitotoxicity and neuroprotection by PSD-95 inhibitors. J Neurosci. **27**, 9901-9915

FIGURE LEGENDS

Figure 1 Purification of CIPP PDZ interactors from mouse brain extracts
Protein staining of two representative 12% acrylamide SDS-PAGE showing position (arrows) of bands present only in the experimental lanes and not in control GST lanes. Numbers near the arrows correspond to representative samples analysed by MS and listed in Table 1. All the other detectable bands of similar molecular weight present in both lanes (control and experiment) were also excised and analyzed via MALDI-TOF PMF for non-specific interactors identification. Typical results obtained using as bait: CIPP-PDZ1 (A) or CIPP-PDZ2 (B).

Figure 2 Analysis of CIPP-PDZ direct interactions
(A) Pull down analysis. Extracts of HEK 293T cells, transiently transfected with FLAG-CNP, FLAG-Cypin and FLAG-IRSp53 respectively, were incubated with GST alone, GST-PDZ1 or GST-PDZ2. Bound proteins were analyzed on 12 % acrylamide SDS-PAGE and detected by immunoblotting using anti-FLAG antibody. Input: 5% of transfected cell extract was loaded on gel. CIPP-PDZ1 specifically bind to FLAG-Cypin; CIPP-PDZ2 to FLAG-CNP and FLAG-IRSp53. (B) Co-immunoprecipitation of FLAG-tagged interactors with full-length GFP-CIPP. HEK 293T cells were transiently transfected with either GFP-CIPP or GFP alone, together with FLAG-IRSp53, FLAG-Cypin, FLAG-CNP or FLAG-vector. Cells extracts were then incubated with ANTI-FLAG® M2 Affinity Gel. Immunoprecipitated were separated on a 10% acrylamide SDS-PAGE and detected by immunoblotting using anti-GFP and anti-FLAG antibodies. Input: 5% of transfected cell extract used for the immunoprecipitation (IP).

Figure 3 Ectopic expression of GFP-CIPP and its FLAG-tagged interactors
HEK 293T cells were transfected with GFP-CIPP (A) (green fluorescence), and with FLAG-Cypin (B), FLAG-CNP (C) and FLAG-IRSp53 (D), detected using anti-FLAG (red staining). Double transfection of GFP-CIPP with Cypin (panels E) shows overlapping localization; co-transfection of GFP-CIPP with CNP (panels F) highlights a partial co-localization, but green staining is still diffused in the cytoplasm. In contrast, co-transfection with FLAG-IRSp53 induces CIPP redistribution and formation of punctate structures dispersed in cytosol and in filopodia (panels G). Localization at the protrusion tips is particularly evident in images shown in panels H. Scale bar: 10 μm in A-G; 2 μm in H.

Figure 4 GFP-CIPP/FLAG-IRSp53 derived puncta occur also in neuronal-like cells
PC12 rat pheochromocytoma cell, induced to a neuronal phenotype by NGF incubation were transfected with GFP-CIPP (A) and FLAG-IRSp53 (B). Only when both constructs were co-expressed puncta formation was observed (panels C). Similar effect in HN9.10e neuroblastoma cell line transfected with GFP-CIPP (D), with FLAG-IRSp53(E), with both constructs (panels F).

Figure 5 The PDZ motif at the extremity of IRSp53 is essential for puncta formation In HEK 293T
Co-transfection of GFP-CIPP with FLAG-C-mut-IRSp53, a mutant of IRSp53 lacking the PDZ binding motif, is still able to induce filopodia protrusions (arrowhead) but does not cause the formation of detectable puncta (panels A). In contrast, co-transfection with FLAG-N-mut-IRSp53, missing IMD and partial CRIB domain, induces large puncta formation but no filopodia protrusions (panels B). Representative cells are depicted. Scale bar: 10 μm.
Co-immunoprecipitation analysis of CIPP with IRSp53 mutants. HEK 293T cells were transfected with either GFP-CIPP or GFP alone, together with FLAG-IRSp53-wt, with FLAG-C mut IRSp53 (C) or with FLAG- N mut IRSp53 (D). Bound proteins were analyzed on 12 % acrylamide SDS-PAGE and detected by immunoblotting using anti-FLAG or anti-GFP antibodies. Input: 5% of transfected cell

extract was loaded on gel.

Figure 6 Cypin is included in CIPP-IRSp53-derived puncta
HEK 293T cells were transfected with HA-Cypin together with GFP-CIPP (panels A) or with FLAG-IRSp53 (panels B). Triple transfection with the three constructs GFP-CIPP, FLAG-IRSp53 and HA-Cypin is showed in panels C. The presence of GFP-CIPP is detected by green fluorescence; HA-Cypin by anti-HA (red staining); FLAG-IRSp53 by anti-FLAG (green staining). Scale bar: 10 μm.

Figure 7 Punctate structures deriving by CIPP-IRSp53 interaction do not colocalize with membrane vesicles
Panel (1): HEK 293T cells co-transfected with FLAG-IRSp53 and GFP-CIPP (green fluorescence) were *in vivo* labelled with dextran-red, to label macropinosomes (A), with transferrin-rhodaminated, to label early and recycling endosomes (B), with lysotracker, to label lysosomes (C). Right panels show an enlargement of the regions outlined by the boxes in the merge panels. Panel (2): fixed HeLa cells co-transfected with FLAG-IRSp53 and GFP-CIPP (green fluorescence) were immunostained with anti-EEA1 antibody to label endosomes (D), with anti-clathrin to label clathrin-coated vesicles (E), with anti-Lamp2 to label lysosomes (panel F), with anti-giantin to label Golgi apparatus (G). Right panels as above. Notably, red and green fluorescence never co-localized in merged images (A to G). Scale bar: 10 μm.

Biochemical Journal Immediate Publication. Published on 13 Jan 2009 as manuscript BJ20081387

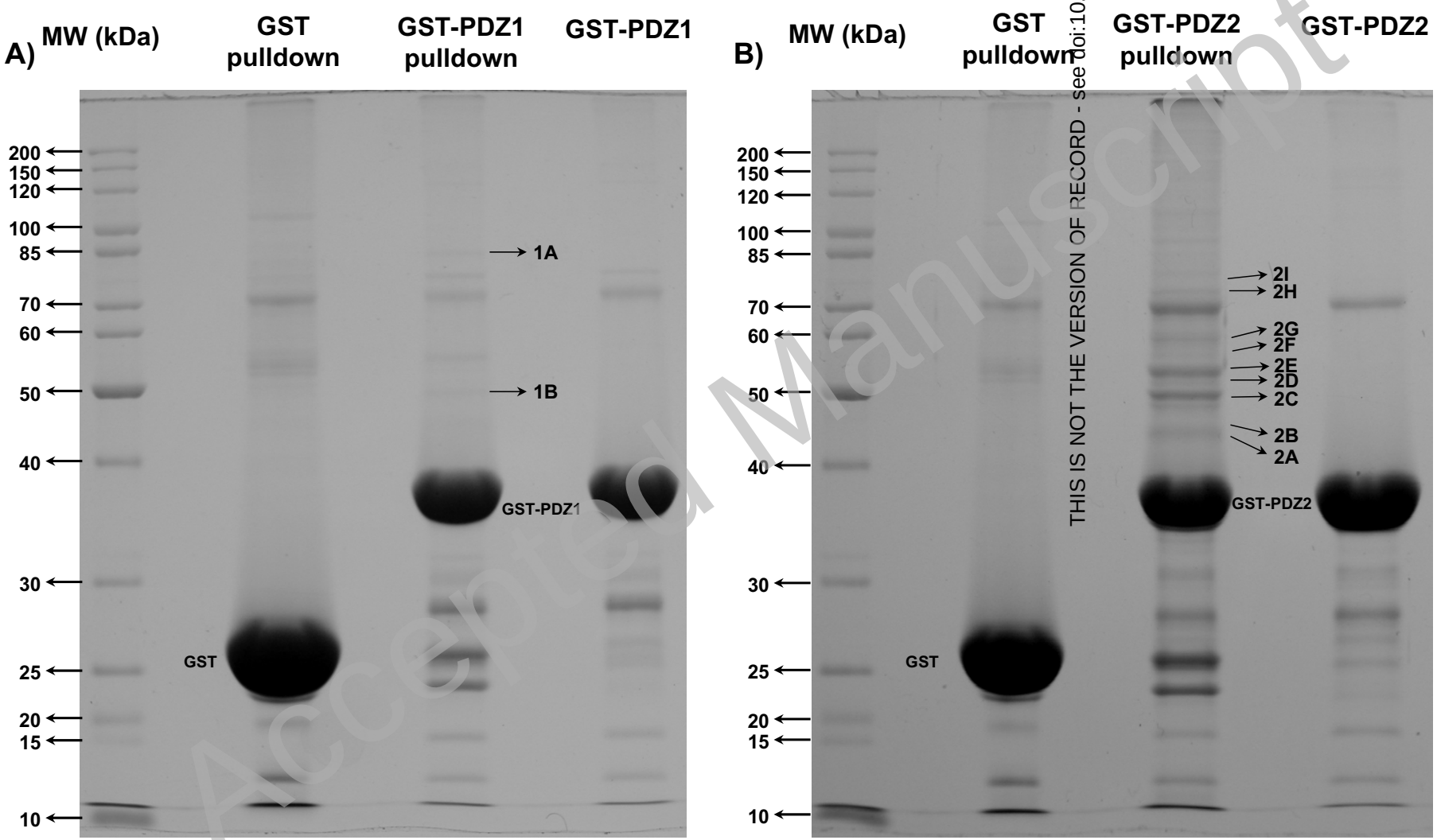

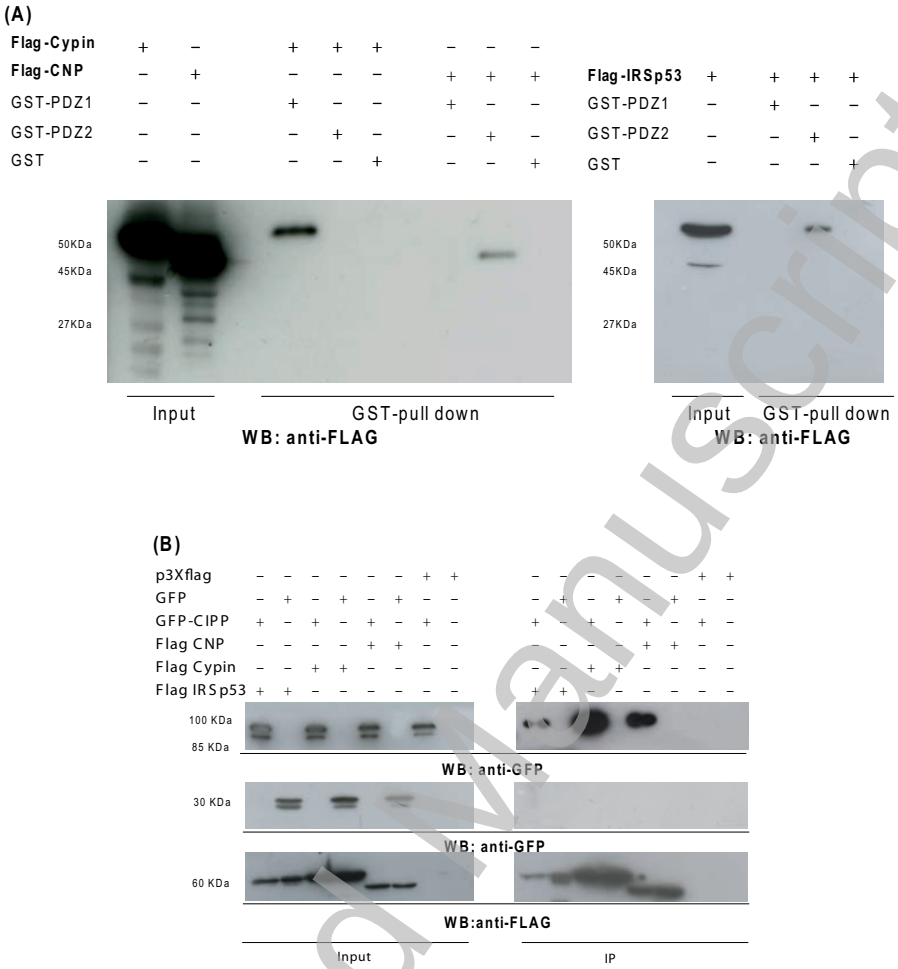

Biochemical Journal Immediate Publication. Published on 13 Jan 2009 as manuscript BJ20081387

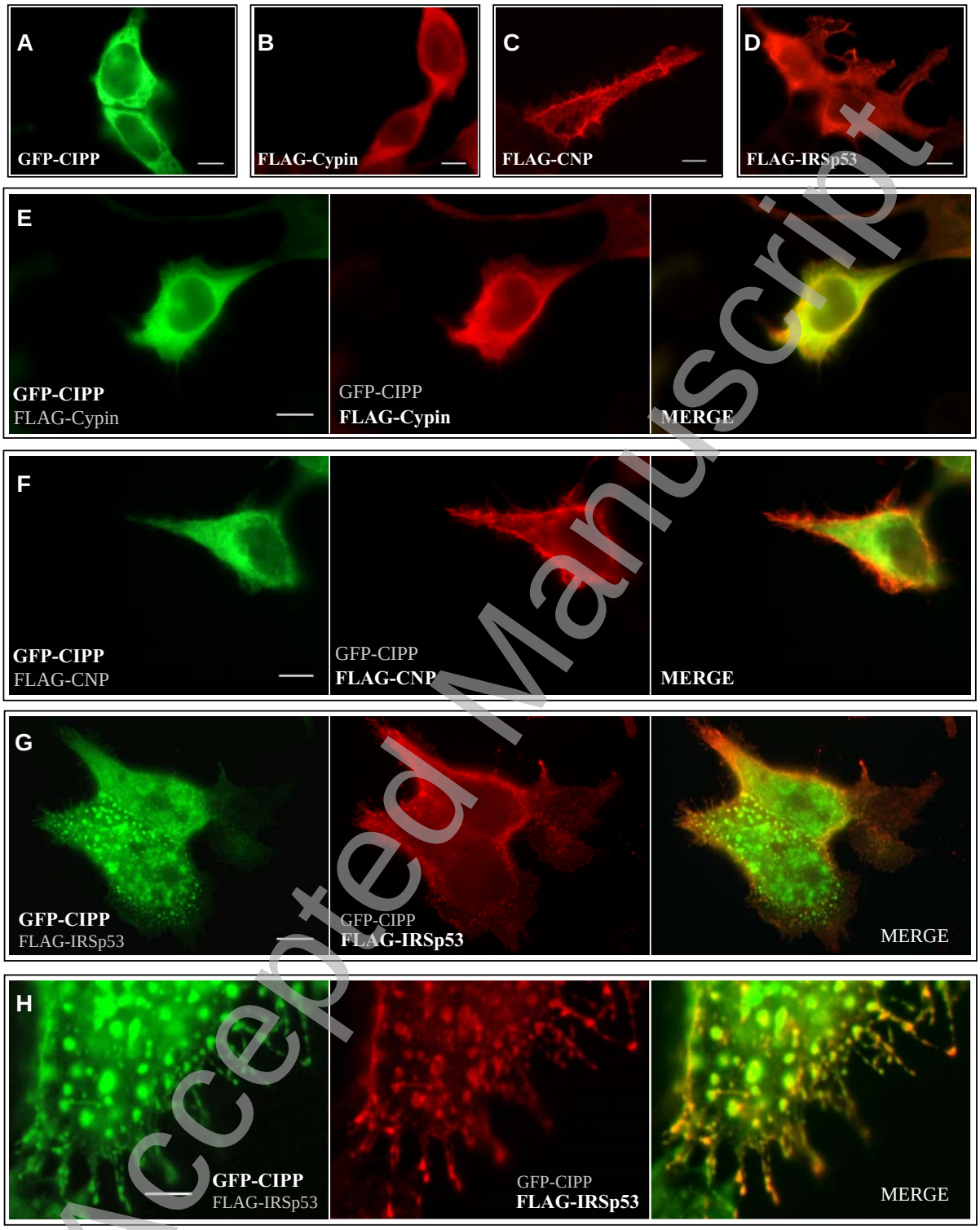

Biochemical Journal Immediate Publication. Published on 13 Jan 2009 as manuscript BJ20081387

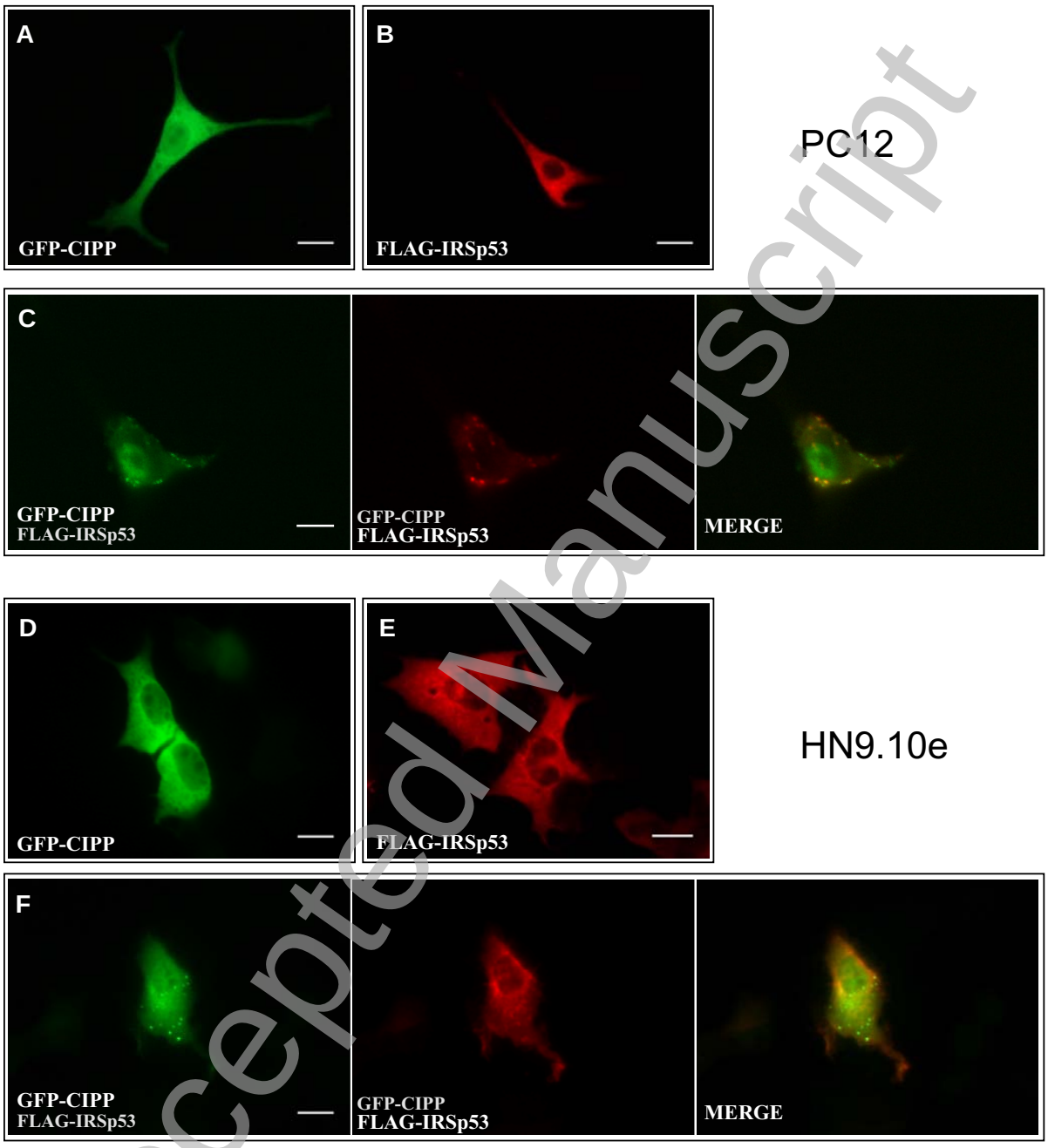

Biochemical Journal Immediate Publication. Published on 13 Jan 2009 as manuscript BJ20081387

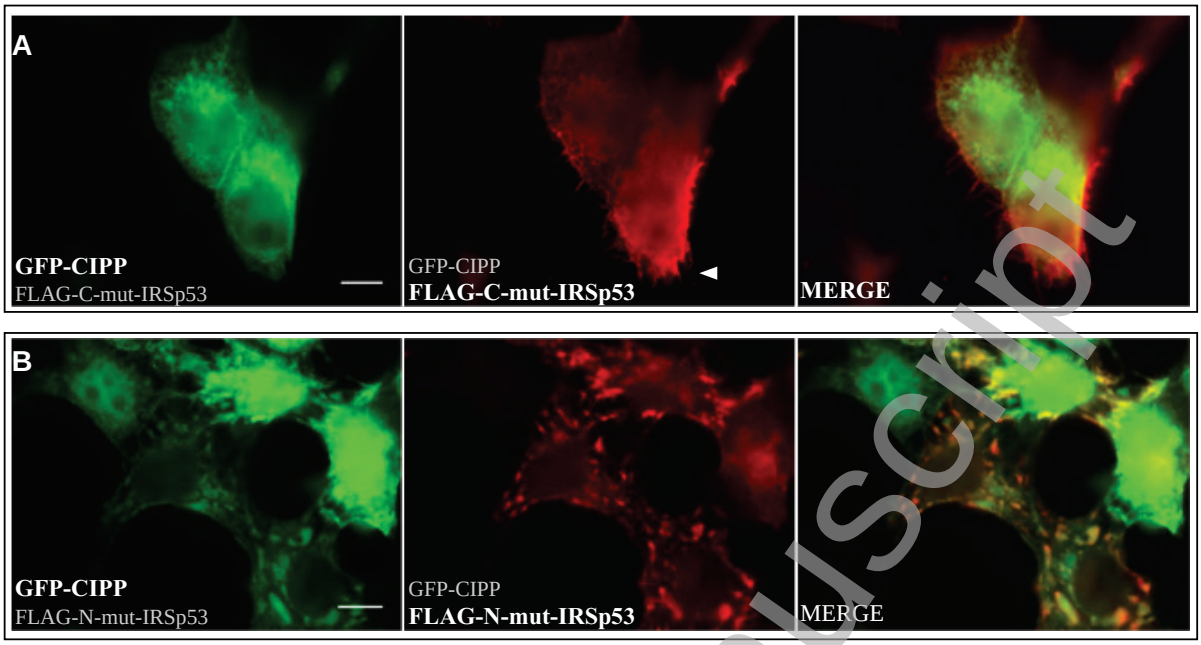

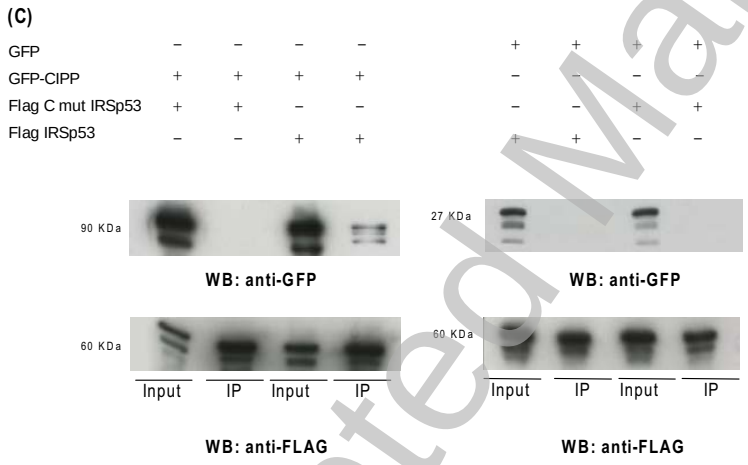

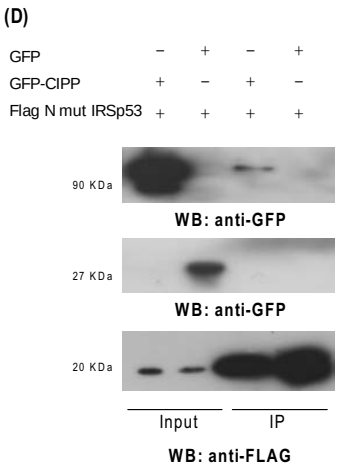

Biochemical Journal Immediate Publication. Published on 13 Jan 2009 as manuscript BJ20081387

10.1042/BJ20081387

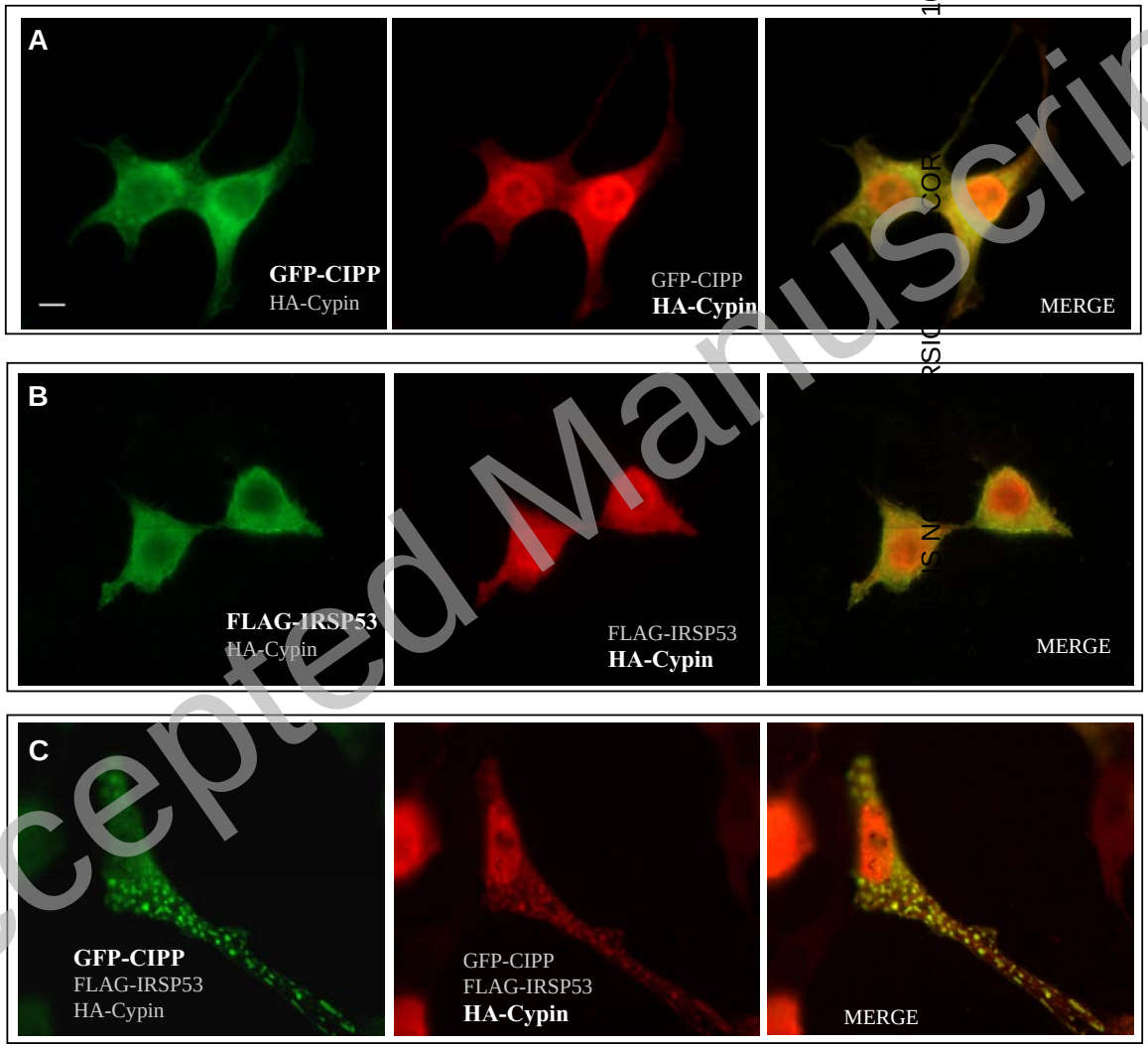

Biochemical Journal Immediate Publication. Published on 13 Jan 2009 as manuscript BJ20081387

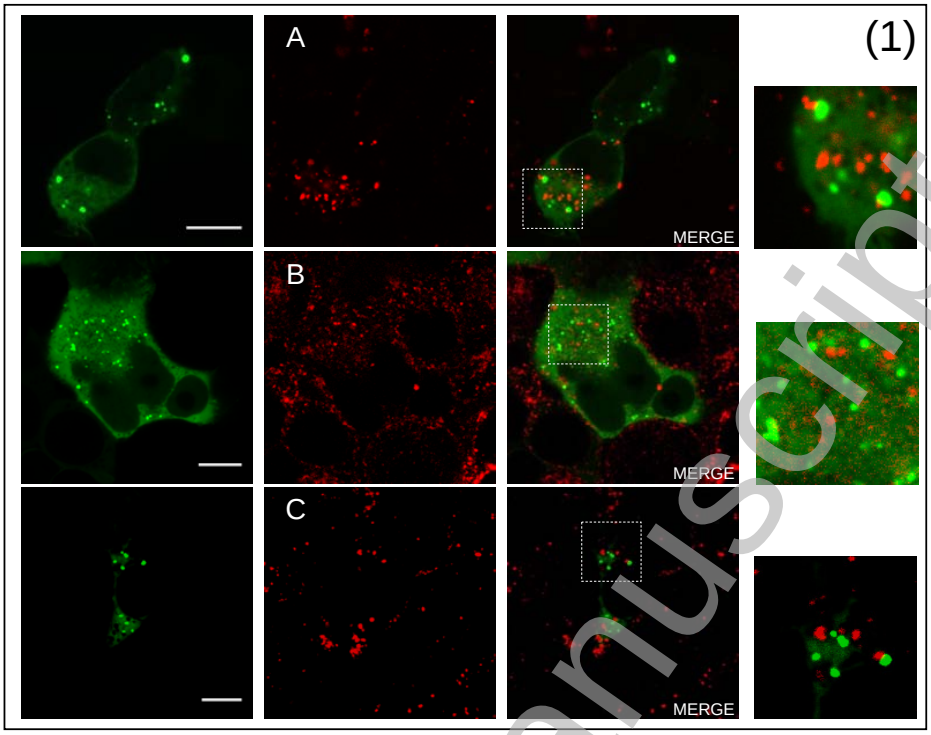

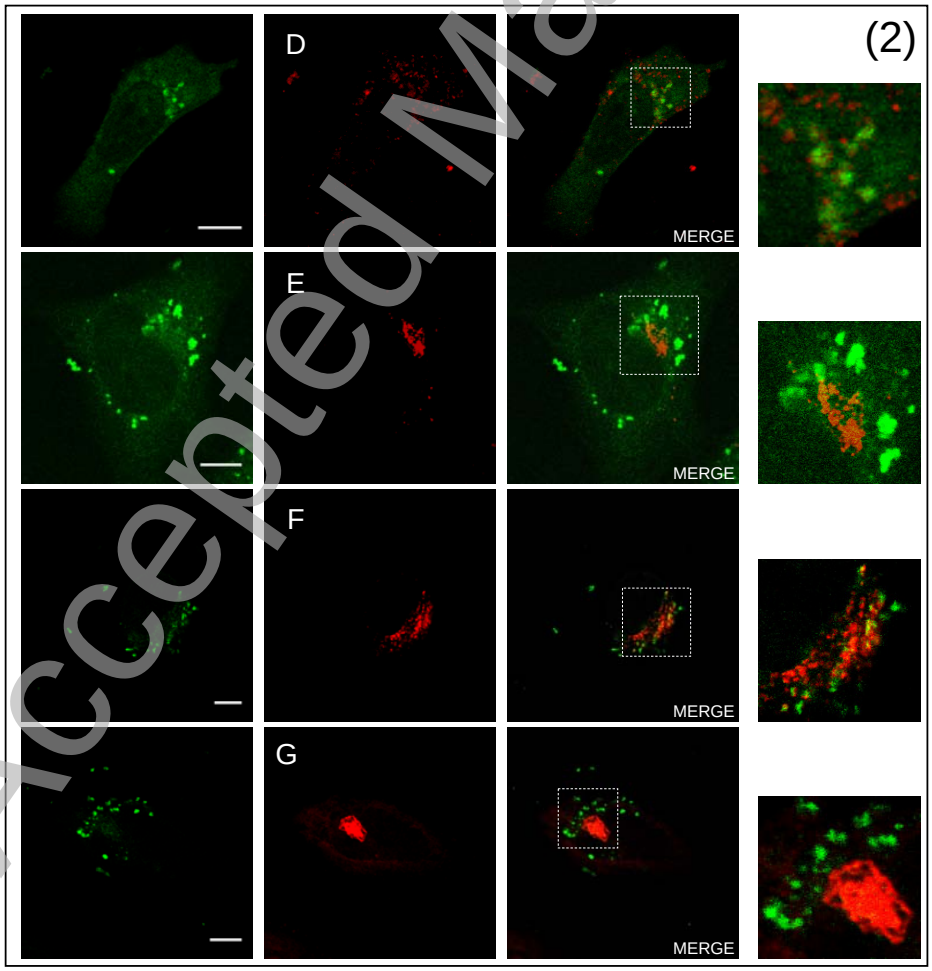

Table 1 Proteins selected by CIPP PDZ domains and identified by MALDI-TOF PMF

N.: samples corresponding to purified bands excised from gels shown in Fig. 1. ***Accession*** refers to UniProt accessions numbers. ***Score*** refers to Mascot probability based MOWSE scoring. ***S.C.***: Sequence coverage is indicated as percent of the entire aminoacidic sequence of the identified protein. ***M.P.***: number of matched peptides. ***M.W.***: molecular weight in kDa. **e-value** refers to expectation values: given a search term, the e-value reflects the number of matches expected to be found by chance in a database; for a given score S of a match, it evaluates the number of hits in a database expected to happen by chance with a score at least equal to S; the e-value takes into account the size of the database that was searched; the lower the e-value, the more significant the score.

CIPP-PDZ1 interactors								
N.	***Identified protein***	***Taxonomy***	***Accession***	***Score***	***S.C.***	***M.P.***	***M.W.***	***e-value***
1A	Protein kinase C beta type (PKC-β)	M. *musculus*	P68404	169	32	21	77	$9.3 \cdot 10^{-13}$
1B	Guanine deaminase (Cypin)	M. *musculus*	Q9R111	178	51	20	51	$1.2 \cdot 10^{-13}$
CIPP PDZ2 interactors								
N.	***Identified protein***	***Taxonomy***	***Accession***	***Score***	***S.C***	***M.P***	***M.W***	***e-value***
2A	Actin, cytoplasmic 1	M. *musculus*	P60710	104	39	15	42	$2.9 \cdot 10^{-6}$
	2',3'-cyclic-nucleotide 3'-phosphodiesterase (CNP)	M. *musculus*	P16330	91	37	15	47	$5.3 \cdot 10^{-5}$
	Glutathione S-transferase class-mu 26 kDa isozyme (GST)	S. *japonicum*	P08515	81	34	8	25	$2.5 \cdot 10^{-3}$
2B	Creatine kinase B-type	M. *musculus*	Q04447	81	38	12	43	$5.6 \cdot 10^{-4}$
2C	Calcium/calmodulin-dependent protein kinase type II alpha chain (CaMKII)	M. *musculus*	P11798	243	47	26	54	$3.7 \cdot 10^{-20}$
2D	ATP synthase subunit beta, mitochondrial precursor	M. *musculus*	P56480	125	40	17	56	$5.0 \cdot 10^{-9}$
	Calcium/calmodulin-dependent protein kinase type II alpha chain (CaMKII)	M. *musculus*	P11798	77	21	12	54	$3.1 \cdot 10^{-4}$
	Tubulin alpha-1C chain	M. *musculus*	P68373	51	23	8	50	$1.4 \cdot 10^{-1}$
2E	Tubulin beta-2A chain	M. *musculus*	Q7TMM9	178	56	30	50	$3.1 \cdot 10^{-14}$
	Tubulin alpha-1A chain	M. *musculus*	P68369	123	53	22	50	$7.9 \cdot 10^{-9}$
	ATP synthase subunit alpha, mitochondrial precursor	M. *musculus*	Q03265	69	35	18	60	$1.8 \cdot 10^{-3}$
2F	Calcium/calmodulin-dependent protein kinase type II beta chain (CaMKII)	M. *musculus*	P28652	153	35	20	60	$3.7 \cdot 10^{-11}$
	Brain-specific angiogenesis inhibitor 1-associated protein 2 (IRSp53)	M. *musculus*	Q8BKX1-2	99	39	15	58	$8.7 \cdot 10^{-6}$
2G	Calcium/calmodulin-dependent protein kinase type II beta chain (CaMKII)	M. *musculus*	P28652	182	39	21	60	$4.6 \cdot 10^{-14}$
	Serine/threonine-protein phosphatase 2B catalytic subunit alpha isoform (CALNA)	M. *musculus*	P63328	55	18	9	59	$2.6 \cdot 10^{-1}$
2H	Heat shock cognate 71 kDa protein	M. *musculus*	P63017	165	30	18	71	$2.3 \cdot 10^{-12}$
2I	Heat shock protein HSP 90-beta	R. *norvegicus*	P34058	159	36	25	83	$6.7 \cdot 10^{-12}$